

Article

CFD Analysis and Validation of a Foreign Material Winnowing Machine for Pepper Harvester

Seo-Yong Shin ¹ , Myoung-Ho Kim ^{1,2}, Yongjin Cho ^{1,2,*}  and Dae-Cheol Kim ^{1,2,*}

¹ Department of Bioindustrial Machinery Engineering, Jeonbuk National University, Jeonju 54896, Korea; ssy9970@naver.com (S.-Y.S.); myoung59@jbnu.ac.kr (M.-H.K.)

² Institute for Agricultural Machinery & ICT Convergence, Jeonbuk National University, Jeonju 54896, Korea

* Correspondence: chojy@jbnu.ac.kr (Y.C.); dckim12@jbnu.ac.kr (D.-C.K.)

Abstract: The winnowing machine of chili pepper harvesters was developed to reduce the potential problem of low pepper stem and fruit separation. The developed winnowing machine was combined with two impellers and a center bearing to prevent a strain on the drive shaft and to ensure durability. The terminal velocity of chili pepper was measured, and an aerodynamic analysis was conducted based on this winnowing machine. A CFD (Computational Fluid Dynamics, Ansys Fluent 2020 R1) analysis was conducted for three levels of discharge port guide form (0, 3, and 5 guides) and three levels of rotating speed (1600, 1800, and 2000 RPM) of a winnowing machine designed utilizing aerodynamic analysis results. A validation test was conducted by fabricating a winnower test device. As for aerodynamic analysis conducted using measured values of terminal velocity, chili pepper fruits were collected at an outlet wind speed lower than 17.5 m/s and chili pepper branches were separated at a speed higher than 12.5 m/s. As a result of CFD analysis, the wind speed deviation at outlets of the 0-, 3-, and 5-guide depending on the rotating speed appeared to be 15.8, 1.4, and 1.0 m/s on average, respectively. The result of the CFD analysis showed values higher than wind speeds of the actual winnower test device by a minimum of 0 and a maximum of 2.4 m/s. Through the CFD analysis and the wind speed validation test of the winnower test device, optimal conditions to separate foreign materials were found to be a winnowing machine at a rotating speed of 1800 RPM with a discharge port having three guides or a winnowing machine at a rotating speed of 2000 RPM with a discharge port having five guides.

Keywords: CFD (Computational Fluid Dynamics); terminal velocity; winnowing machine separation; chili pepper harvester



Citation: Shin, S.-Y.; Kim, M.-H.; Cho, Y.; Kim, D.-C. CFD Analysis and Validation of a Foreign Material Winnowing Machine for Pepper Harvester. *Appl. Sci.* **2022**, *12*, 6134. <https://doi.org/10.3390/app12126134>

Academic Editors: Pawel Kielbasa, Tadeusz Juliszewski and Sławomir Kurpaska

Received: 19 May 2022

Accepted: 14 June 2022

Published: 16 June 2022

Publisher's Note: MDPI stays neutral with regard to jurisdictional claims in published maps and institutional affiliations.



Copyright: © 2022 by the authors. Licensee MDPI, Basel, Switzerland. This article is an open access article distributed under the terms and conditions of the Creative Commons Attribution (CC BY) license (<https://creativecommons.org/licenses/by/4.0/>).

1. Introduction

As a vegetable crop, chili pepper has an output ranked the seventh largest among vegetables globally. It contains capsaicin with a spicy taste. It is widely used as an industrial material and a seasoning ingredient for various foods. Major chili pepper-producing countries are China, India, Thailand, Bangladesh, Myanmar, Vietnam, USA, Peru, and Korea, most of which are concentrated in Southeast Asia [1]. Chili pepper is the second most important crop for farm household income after rice in Korea. It is an important seasoning vegetable that accounted for 33% of condiment vegetables in 2020. However, its cultivation area and output are decreasing due to the aging of chili pepper growing farms, low mechanization rate, and labor cost burden with an increase in the production cost. It has been reported that chili pepper cultivation area, output, and production cost per 10a of Korea have been changed from 74,471 ha, 193,786 tons, and 1,126,000 KRW in 2000 to 31,146 ha, 60,076 tons, and 3,707,000 KRW in 2020, respectively. Additionally, the report showed decreases of 41.8%p and 31.0%p in cultivation area and output, and an increase of 329.2%p in production cost [2,3].

The chili pepper harvesters have been researched and developed in many countries to increase chili pepper cultivation area and output [4–6]. As additional human resources are

put in to separate foreign materials because existing chili pepper harvesters have a high rate of foreign materials in the collection tank after harvest, the foreign material separation system needs to be improved [7–10]. The separation of small chili pepper branches, leaves, soil, and so on that are moved to the collection section during mechanical harvesting of chili pepper occupies an important part of low transportation cost, processing cost, and simplification of the post-treatment process [11–13]. As a result of developing a small size chili pepper harvester and conducting a performance comparison test, Kim et al. [14] have reported foreign material adulteration rates of 17.6 to 31.0% on average and presented the necessity for a foreign material separation device to reduce additional separation workforce after harvest. Studies on the separation of foreign materials use the method where foreign materials are separated by square plates installed at a constant interval on a rotating shaft and the winnower method where foreign materials are separated using the air based on the difference in terminal velocity crop. In a study on rotating square plates, Lenker et al. [15] have removed 65% of foreign materials by putting harvested chili pepper on a wire belt with a number of 3.1-cm high fingers installed at an interval of 2.5 cm and making small chili pepper branches and leaves fall through the space between the fingers while the belt vibrates and rotates. Wolf et al. [16] have removed 42% of foreign materials due to fabricating three star-shaped star wheels that rotate in a single direction and one square rubber plate and using them to separate seeds, small branches, and leaves. Eaton et al. [17] have achieved chili pepper separation rates of 90% to 95% and a foreign material separation rate of 93.5% under conditions of a rotating card cleaner size of 6 inches, an interval of 22.2 mm, an inclination angle of 20°, and rotating speeds of 50 to 100 RPM after mechanical harvesting of a chili pepper species cultivated in New Mexico State. Kong et al. [18] have conducted a test after designing and fabricating a separation system using star wheels and air current based on morphological features and aerodynamic characteristics of a chili pepper species cultivated in Xinjiang, China. When the interval of star wheel plates was 108 to 200 mm and the distance between shafts was 180 to 200 mm, it was found that 29.5% of branches and 75.0% of foreign materials were separated. Jo et al. [19] designed and fabricated a card cleaner device and conducted a performance test. As a result of the test, the foreign material separation rate was 53.5% under a straight-line card arrangement, an inclination angle of 15°, and a rotation speed of 50 RPM. Statistical analysis showed that the foreign material separation rate was significantly related to the inclination angle and the rotating speed. Byun et al. [20] have established optional conditions of a card cleaner device by grasping its mechanical and physical properties using the discrete element method (EDEM) and found that conditions are similar to those of the factorial performance experiment of Jo et al. [19].

In a study on the aerodynamic winnowing method, Bilanski et al. [21] have experimentally obtained and induced terminal velocity of freely falling grains using a time-displacement technique to measure terminal velocities of seven kinds of grains and seeds such as wheat about that of a plastic sphere. In an aerodynamic study on the air stream separation of grains, Lee et al. [22,23] analyzed the effect of rice and barley sizes and moisture content on the measurement of terminal velocity. Their measurement results showed that the terminal velocity of rice was 4.6 to 4.8 m/s and that of barley was 4.9 to 5.5 m/s. Chung et al. [24] have experimentally investigated aerodynamic characteristics of the separation section in a combine. As a result of making measurements at a winnower rotating speed of 1150 RPM, it was found that air separation of wheat, branch straw, and leave straw was possible at 4.1 m/s, 2.4 m/s, and 1.3 m/s, respectively. To confirm the physical, mechanical, and aerodynamic properties required for separation after the mechanical harvesting of peanuts, Kim et al. [25] have compared the results of a modeling calculation and an actual test. Their test results showed that the breaking power of peanut hulls was irrelevant to their shape, size, or moisture content, with a drag coefficient range of 0.67 to 0.93. Choi [26] has conducted a test after fabricating a device to separate chili pepper using a winnowing fan and a vibrating separation sieve. As a result of the separation, the chili pepper separation rate was 68.2% when the wind speed of the winnowing machine was 6.2 m/s, the

frequency of the separating sieve was 6.9 Hz, the amplitude was 40 mm, and the thickness and interval of the separation sieve rods were 6 mm and 29 mm, respectively. As a result of conducting a test of removing foreign materials from chili peppers by organizing a fan absorption winnowing device, a discharge conveyor, and a foreign material collecting bin, Hong et al. [27] have found that chili pepper leaves are absorbed in a winnowing machine wind speed of 12 to 15 m/s and the foreign material removal rate is 95%. Noh et al. [28] have evaluated the separation rate and loss rate at the foreign material separation winnowing machine's rotation speed of 180 to 300 RPM to develop a sesame harvester. As a result of the test, separation rates of sesame were 99.7% and 99.8% at 220 and 240 RPM, respectively. These were reported as the optimal RPMs of the winnowing machine with the least loss.

Lee et al. [29] have analyzed the fluid flow of a peanut harvester's winnowing machine by conducting a CFD analysis. They found that the fluid flow was adequate when the direction was counterclockwise and the rotating speed and the flow field velocity were 1500 RPM and 8 to 17 m/s, respectively. The separation system of the peanut harvester was investigated in a factor experiment using the analyzed result [30]. Yuan et al. [31] have analyzed the separation performance using the CFD-DEM (Computational Fluid Dynamics—Discrete Element Method model) to improve the separation performance of a combine and save the cost. Separation and performance efficiencies were 98.9% and 87.7%, respectively, at a wind speed of 11.0 m/s. The error in the separation rate was 5% or less. Those in the loss rate and separation efficiency were 9.8% and 2.6%, respectively, through the analysis result and validation test. Shin et al. [32] have designed and fabricated a winnower test device for a chili pepper harvester and conducted a performance test. The conditions that achieved the least loss of chili pepper and the highest separation rate of foreign materials were a winnower inclination angle of 34° and a rotating speed of 2000 RPM. Winnowing machines presented in the existing literature showed the following trend: the higher the rotating speed of the winnowing machine, the larger the loss of chili pepper fruit and the higher the foreign material separation rate. It is required to find a way to minimize the loss of chili pepper fruits and secure adequate foreign material separation at the same time. The optimization and application of CFD solution were studied to evaluate fluid flow around a target object at a low Reynolds number and numerical study on the drag coefficient. Additionally, the CFD simulation was used to evaluate the flow patterns and indicate the important numerical solutions. To optimize parameters of winnowing equipment for machine-harvested *Lycium barbarum* L., a discrete element method (DEM) simulation of ripe fruit in the airflow was performed using EDEM software [33]. Aerodynamic analysis and CFD simulation were conducted to evaluate the model on temperature and relative humidity or predict the terminal velocity of agricultural granular materials or perform the wind tunnel in the agriculture field [34–36].

Thus, the objective of the present study was to design a foreign material separation winnowing machine for specializing work in chili pepper harvesters through an aerodynamic analysis and validate the same using CFD (Computational Fluid Dynamics, Ansys Fluent 2020 R1) software. Detailed objectives are below.

1. The first objective is to measure the terminal velocities of chili pepper species and conduct an aerodynamic analysis. The terminal velocities of chili pepper fruit, chili pepper stem, and chili pepper leaf move distance by wind are each derived through aerodynamic analysis.
2. The second objective is to validate the winnowing machine through a CFD analysis and test device. The wind speed of CFD flow analysis is verified as a flow test of separation equipment. In this result, the optimal rotation speed and discharge out guides for foreign material separation are decided, which will be applied to the chili pepper harvester.

2. Materials and Methods

2.1. Aerodynamic Properties of Mechanically Harvested Chili Pepper

In the present study, species ‘Jeokyoung’ and ‘AR Legend’ were selected. Terminal velocities of their chili pepper fruits, chili pepper branches, and chili pepper leaves were measured. ‘Jeokyoung’ and ‘AR Legend’ are species with large fruits developed by the National Institute of Horticultural and Herbal Science (NIHHS). They have high chromaticity, lots of chili pepper fruits, and strong resistance against diseases and pests such as anthrax bacterium. These chili peppers were transplanted from an NIHHS experimental field on 8 May 2019. Measurements were made on 18 August 2019 (after 103 days) during the harvesting period.

2.2. Terminal Velocity Measurement

The terminal velocity of the chili peppers was measured by controlling the wind speed. Chili pepper fruits and chili pepper branches were put in a floating state at the height of 10 to 20 cm using an upward air current with a uniform velocity [37,38]. Figure 1a shows the look of the terminal velocity device used for the test. Figure 1b shows the wind speed meter used. As for the measurement method, velocity values were measured by inserting the hot wire probe of a wind speed meter into the hole of the transparent tube with the chili pepper fruits and chili pepper branches in a floating state [19,20]. Each chili pepper fruit and chili pepper branch were collected 10 times, and the average value and standard deviation were calculated by three repetitions of the test. Detailed specifications of the wind speed meter used for the test are shown in Table 1. Table 2 shows the results of measuring terminal velocities of chili pepper fruits, chili pepper branches, and chili pepper leaves.

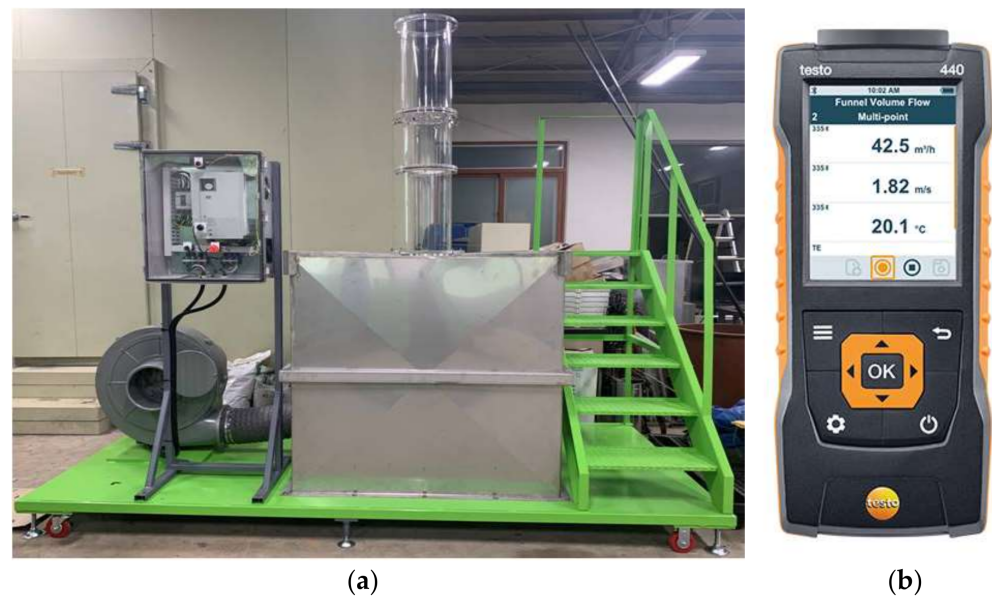


Figure 1. Terminal velocity experiment bench (a) and wind velocity measuring instrument (b).

Table 1. Specifications of wind velocity measuring equipment.

Item	Specification
Model number	TESTO 440
Company/Nation	TESTO/GERMANY
Measuring range	0–30 m/s
Resolution	0.1 m/s
Accuracy	0.04%

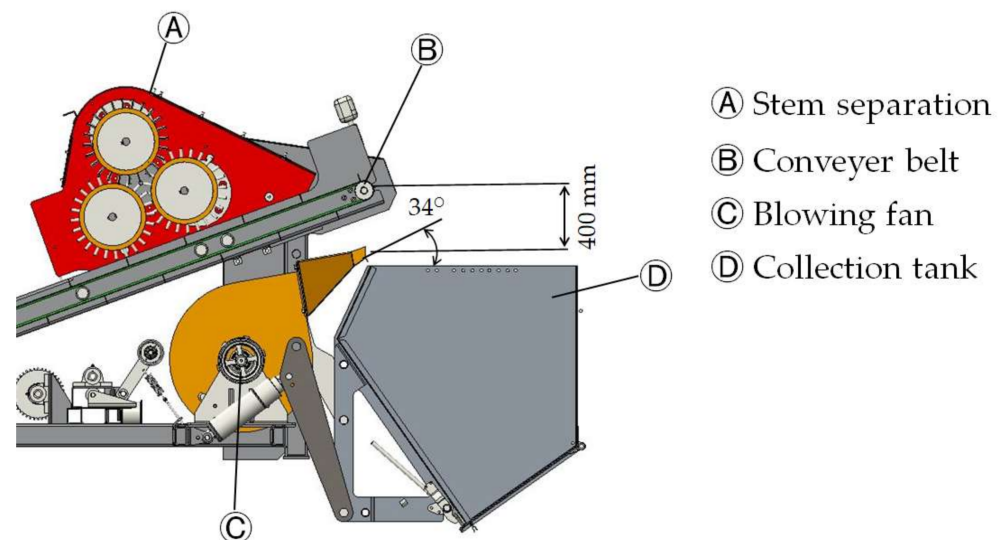
Table 2. Experiment results of pepper terminal velocity.

Pepper Part	Variety	V_t ¹ (m/s)	
		AVE ²	SD ³
Fruit	Jeokyoung	13.7	1.1
	AR legend	13.5	0.4
Branch	Jeokyoung	11.2	0.5
	AR legend	11.5	1.6
Leaf	Jeokyoung	4.3	0.5
	AR legend	4.2	0.2

¹ V_t : terminal velocity; ² AVE: average; ³ SD: standard deviation.

2.3. Aerodynamic Analysis of Winnowing

The chili pepper harvester developed by Shin et al. [10,32] was arranged to separate foreign materials such as chili pepper branches and chili pepper leaves and collect only the harvested chili pepper fruits in a collection tank. Figure 2 shows the construction of the foreign material winnowing system developed by Shin et al., in addition to the chili pepper harvester [10,32] they developed. It is organized to transfer harvested chili pepper fruits and foreign materials such as chili pepper branches and leaves to a conveyor belt and separate foreign materials outside of the collection tank by the wind of the winnowing machine when they fall into the collection tank. Terminal velocities of chili pepper fruit, chili pepper branch, and chili pepper leaf were set to be 13.5, 11.5, and 4.2 m/s, respectively, using the terminal velocity measurement result. Chili pepper leaf was excluded from the aerodynamic analysis considering it could be separated at a wind speed lower than that of a chili pepper branch. In the aerodynamic analysis of winnowing, travel distances of chili pepper fruits and chili pepper branches with time were derived from the wind speed discharged at an inclination angle of 34° . At this time, it was assumed that the wind speed was constant only in one direction. If a wind speed is applied to chili pepper fruits and chili pepper branches when they fall freely into the collection tank from a height of 400 mm, forces of drag and gravity are generated in the direction of F_{Dx} , F_{Dy} , mg (Figure 3). F_{Dx} is the drag force moving in the x-axis direction and F_{Dy} is the drag force moving in the y-axis direction. Conditions used to calculate of measured material properties and travel distances are shown in Table 3.

**Figure 2.** Components of a separation system for foreign materials.

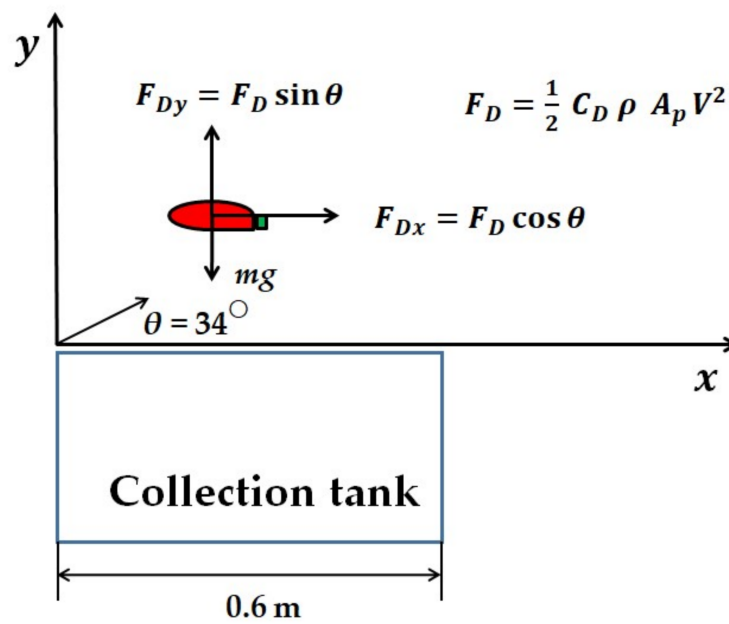


Figure 3. Force acting on the pepper fruit by winnowing machine velocity.

Table 3. Calculation formula parameter for pepper fruit and branch in the blowing fan.

Parameter	Pepper Fruit	Branch	Unit
Length (L_1)	0.11	0.2	m
Diameter (L_2)	0.017	0.004	m
Weight (m)	0.012	0.004	kg
Terminal velocity (V_t)	13.5	11.5	m/s
Air density (ρ)	1.27	1.27	kg/m ³
Acceleration of gravity (g)	9.81	9.81	m/s ²
Velocity (V_{air})	10, 12.5, 15, 17.5	10, 12.5, 15, 17.5	m/s
Winnowing machine angle	34	34	°
x-axis start direction (S_{x0})	0	0	m
y-axis start direction (S_{y0})	0.4	0.4	m
Analysis time interval (t)	0.1	0.1	s

Chili pepper fruit and chili pepper branch are assumed to be aspherical ellipsoids. Therefore, the projected area is shown in Equation (1) [39]:

$$A_p = \frac{\pi L_1 L_2}{4} \tag{1}$$

where A_p = projected area (m²); L_1 = length of object (m); and L_2 = diameter (thickness) of object (m).

When the projected area and terminal velocity value are used, the drag coefficient of chili pepper fruit and chili pepper branch is shown in Equation (2) [39]:

$$C_D = \frac{2 m g}{\rho A_p V_t^2} \tag{2}$$

where C_D = drag coefficient; ρ = air density (kg/m³); V_t = terminal velocity of object (m/s); m = weight of object (kg); and g = acceleration of gravity (m/s²).

The drag applied to chili pepper fruit and chili pepper branch in the x-axis direction, which is expressed using the projected area value as shown in Equation (3) [40]. The acceleration (a_x) applied in the x-axis direction is shown in Equation (4) [40]. The wind speed (V_{air}) is the relative velocity of the chili fruit and chili branch's speed (V_{xp}). When

the initial time (t) is 0, (V_{xp}) becomes 0. The acceleration is assumed to be constant at the analysis time interval of 0.1 s.

$$F_{Dx} = m a_x \quad (3)$$

where F_{Dx} = drag force of x-axis direction (N); and a_x = acceleration of x-axis direction (m/s^2).

$$a_x = \frac{F_{Dx}}{m} = \frac{1}{2} \frac{C_D \rho A_p (V_{air} \cos \theta - V_{xp})^2}{m} \quad (4)$$

where V_{air} = wind velocity (m/s); and V_{xp} = x-axis direction velocity of object (m/s).

The drag applied to chili pepper fruit and chili pepper branch in the y-axis direction is affected by the gravitational acceleration, which is shown in Equation (5) [40]. The acceleration applied in the y-axis direction (a_y) is shown in Equation (6) [40].

$$F_{Dy} = -m a_y + m g \quad (5)$$

where F_{Dy} = drag force of y-axis direction (N); and a_y = acceleration of y-axis direction (m/s^2).

$$a_y = g - \frac{F_{Dy}}{m} = g - \frac{1}{2} \frac{C_D \rho A_p (V_{air} \sin \theta - V_{yp})^2}{m} \quad (6)$$

where V_{yp} = y-axis direction velocity of object (m/s).

Velocities of chili pepper fruit and chili pepper branch in the x-axis direction, V_x , and in the y-axis direction, V_y , are expressed using acceleration values (a_x) and (a_y) and calculated at the analysis time (t) of 0.1 s as shown in Equation (7) [40]. Based on the analysis time (t), the initial velocity (V_{n-1}) of V_x or V_y is the velocity value previously calculated. It becomes the initial value.

$$V_n = V_{n-1} + a_n t \quad (7)$$

where V_n = velocity of an object (V_x or V_y) (m/s); V_{n-1} = previous value for velocity of object (m/s); a_n = acceleration (a_x or a_y) (m/s^2); and t = time interval of analysis (s).

The travel distance in the x-axis direction, S_x , expressed using the acceleration in the x-axis direction and the y-axis direction (a_x , a_y) and velocity (V_x , V_y) values calculated at each time (t) are shown in Equation (8) [40]. The travel distance in the y-axis direction, S_y , is shown in Equation (9) [40]. The initial travel distance S_{x0} is 0 m. S_{y0} is fixed to the fall height of 0.4 m. As to the analysis time (t), the calculation is made at an interval of 0.1 s for up to 5 s.

$$S_x = S_{x0} + V_x t + \frac{1}{2} a_x t^2 \quad (8)$$

where S_x = travel distance of x-axis direction (m) and S_{x0} = initial travel distance of x-axis direction (0 m).

$$S_y = S_{y0} + V_y t + \frac{1}{2} a_y t^2 \quad (9)$$

where S_y = travel distance of y-axis direction (m) and S_{y0} = initial travel distance of y-axis direction (0.4 m).

2.4. Flow Analysis of Winnowing Machine

In this chapter, a flow analysis is conducted based on the rotating speed of the winnower and the shape of the discharge port guide designed using the Ansys FLUENT 2020R1 program, a commercial CFD (Computational Fluid Dynamics) code. The winnower comprised of two impellers was designed in Figure 4 to select an optimal flow field based on the discharge port guide level 3. Detailed data are shown in Table 4.

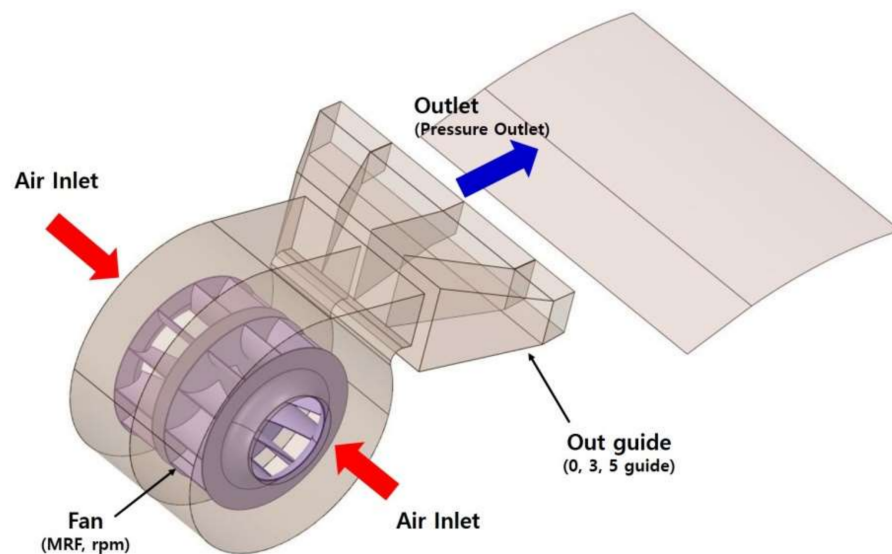


Figure 4. Schematic diagram showing boundary conditions and internal flow field of blowing fan for analysis model.

Table 4. Specifications of the blowing fan model.

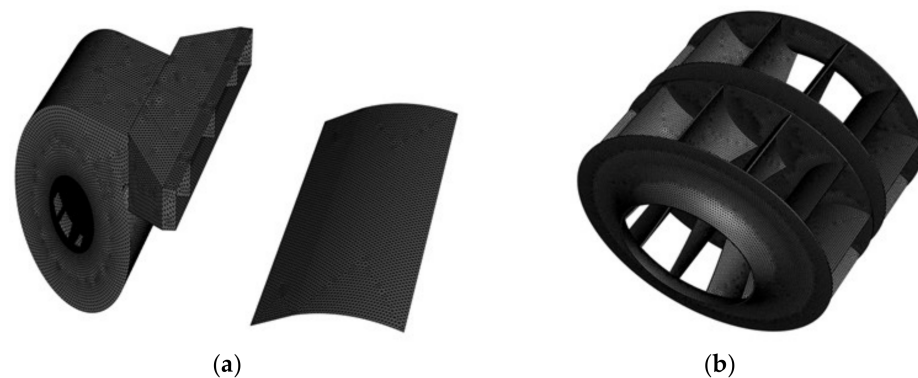
Design Specifications	Value
Model Size: length, width, high (mm)	631 × 510 × 602
Out guide type	0, 3, 5
Impeller	Centrifugal type (2ea)
Impeller: diameter × width × wing number (mm, ea)	330 × 137 × 12

2.5. CFD Modeling and Simulation Setup

In the flow analysis, a coupled-type algorithm with excellent convergence was used. The MRF (Multi Reference Frame) method was used to simulate the rotation of a fan. The CFD numerical analysis procedure was performed in the order of geometry modeling, mesh, physics, solver settings, computing solution, and post-processing. Modification of the model was considered when reviewing the analysis results [41]. Detailed boundary conditions for numerical analysis are shown in Table 5. Depending on the winnower fan rotating speed (1600, 1800, 2000 rpm) and the outlet guide shape (0-, 3-, 5-guide), analysis conditions for the winnower rotating speed and the discharge port guide were set, referring to the reported factorial experiment of the foreign material separation [32,42]. Internal parallel processing with six cores is used to solve the simulation. Regarding the grid system used for the flow analysis, a tetrahedron grid system was applied. It was comprised of a total of 1,259,970 nodes and 5,004,653 grids. The maximum element size for the rotating area is set to 0.002 m. The length of the element at the interface between the fixed and rotating area is set to 0.005–0.01 m. For grid generation, the surface mesh used a triangle, and the volumetric mesh used a tetrahedron and prisms. The satisfy condition with orthogonal quality was 0.1 to 0.2, and the validation with a skewness value was between 0.8 and 0.9. The solver setting was confirmed as the stable state in the conditions of time step 0.5 s and residual 10^{-3} less [43]. The housing of the winnower to which the grid system was applied is shown in Figure 5a. The impeller to which a dense grid system was applied is shown in Figure 5b.

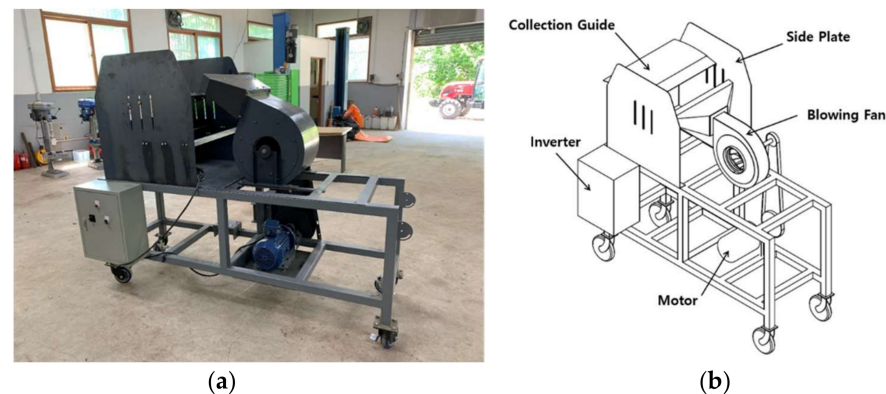
Table 5. Numerical analysis method for boundary conditions.

Parameter	Value
CFD method	Moving reference frame
Fluid	Air
Inlet, outlet	Static pressure
Turbulence model	Standard k-epsilon/Realizable/Standard Wall Functions
Wall	No Slip condition
Mesh Nodes/Elements	1,259,970/5,004,653
Mesh minimum orthogonal quality	0.13
Mesh maximum quality	0.87817363
Time step	0.5 s
Iterations	Hybrid, 500

**Figure 5.** Mesh composition of (a) a blowing fan and (b) the main impeller.

2.6. Fabrication and Evaluation of Widdowing Machine

The test device by discharge port guide that affects the performance of the widdowing system is shown in Figure 6a,b. Depending on the rotating speed of the widdower and the discharge port guide shape, measurements were made at each position using a wind speed meter (TESTO-440, Lenzkirch, Germany).

**Figure 6.** Picture (a) and schematic view (b) of the experiment bench for a separation equipment.

3. Results and Discussion

3.1. Result of Aerodynamic Analysis

Results of calculating the travel distances of chili pepper fruit and chili pepper branch depending on the wind speed at the widdower discharge port are shown in Figures 7 and 8, respectively. Chili pepper fruits are shown in Figure 7a; those which fell freely were found to have been collected in the collection tank at wind speeds of 10.0, 12.5, and 15.0 m/s. At a wind speed of 17.5 m/s, chili pepper fruits were found to have flown outside the collection tank, causing a loss to occur. As for the loss of the chili pepper fruit, it was found that the

moving distance of the pepper fruit was over 0.6 m at a wind speed of 17.5 m/s. Chili pepper branches, as shown in Figure 7b, were found to have been separated, flying out of the collection tank at wind speeds of 15.0 and 17.5 m/s. For the separated chili pepper branches, it was found that the moving distance of pepper branch was over 0.6 m at a wind speed of 15 and 7.5 m/s. As a result of conducting an aerodynamic analysis, it was determined that chili pepper fruits were collected in the collection tank at a wind speed lower than 17.5 m/s. Furthermore, the chili pepper branches were separated to be outside of the collection tank at a wind speed higher than 12.5 m/s.

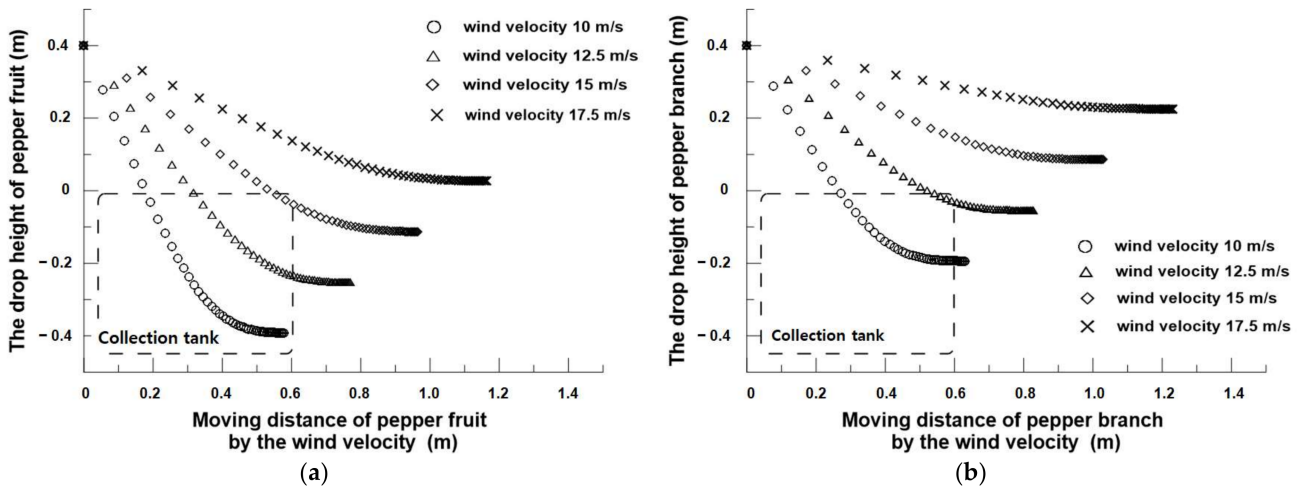


Figure 7. Graph of calculated moving distance for the pepper fruit (a) and the pepper branch (b) by velocity equation.

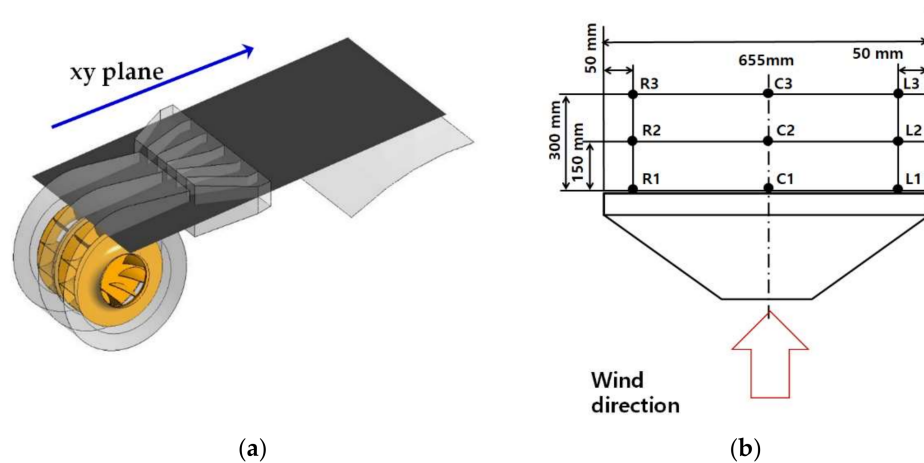


Figure 8. The xy plane on 3D model (a) and measuring position of blower on top view (b).

3.2. Flow Analysis Results

Wind speed measurement positions depending on the shape of the discharge port guide are shown in Figure 8a,b. Drift velocity distributions of the upper xy plane for the discharge port with 0-, 3-, and 5-guide at a winnower rotating speed of 1600 RPM are shown in Figure 9a–c, respectively. As a result of flow field velocity distribution, the 0-guide showed an average of 19.9 m/s at C1 and 4.3 m/s at L1 and R1. The 3-guide showed an average of 17.7 m/s at C1 and 15.9 m/s at L1 and R1. The 5-guide showed an average of 15.5 m/s at C1 and 14.5 m/s at L1 and R1. Flow velocity deviations at the left and right points, L1 and R1, from the center, C1, of the discharge port were shown to be 15.6, 1.8, and 1.0 m/s in the case of the 0-, 3-, and 5-guide, respectively. The velocity deviation of the 5-guide was found to be the least.

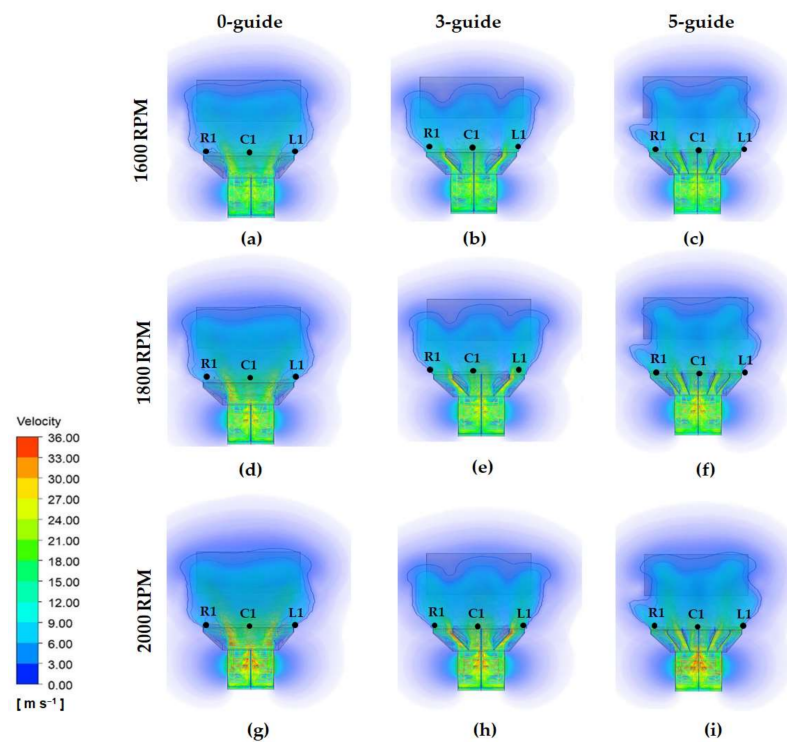


Figure 9. Shape analysis of flow field for foreign materials separating part of xy plane on conditions of 0-guide (a), 3-guide (b), 5-guide (c) at 1600 RPM, 0-guide (d), 3-guide (e), 5-guide (f) at 1800 RPM, and 0-guide (g), 3-guide (h), 5-guide (i) at 2000 RPM.

Figure 9d–f show the flow velocity distributions for the discharge port with 0-, 3-, and 5-guide at a winnower rotating speed of 1800 RPM, respectively. As a result of the flow field velocity distribution, the 0-guide showed an average of 22.6 m/s at C1 and an average of 5.0 m/s at L1 and R1. The 3-guide showed an average of 20.6 m/s at C1 and 23.2 m/s at L1 and R1. The 5-guide showed an average of 19.4 m/s at C1 and 16.7 m/s at L1 and R1. The flow velocity deviations at the left and right points, L1 and R1, from the center, C1, of the discharge port were shown to be 17.7, 2.6, and 2.7 m/s in the case of 0-, 3-, and 5-guide, respectively. The velocity deviation of the 3-guide was found to be the least.

Figure 9g–i show velocity distributions for discharge port with 0-, 3-, and 5-guide at a winnower rotating speed of 2000 RPM, respectively. As a result of the flow field velocity distribution, the 0-guide showed an average of 24.1 m/s at C1 and 5.8 m/s at L1 and R1. The 3-guide showed an average of 22.9 m/s at C1 and 25.6 m/s at L1 and R1. The 5-guide showed an average of 18.6 m/s at C1 and 19.0 m/s at L1 and R1. The flow velocity deviation at the left and right points, L1 and R1, from the center, C1, of the discharge port was shown to be 18.3, 2.7, 0.4 m/s in the case of 0-, 3-, and 5-guide, respectively. The velocity deviation of the 5-guide was found to be the least.

3.3. Results of Comparing Winnower Speed Measurement and Flow Analysis

Results of measuring wind speeds in the winnower test device and wind speeds determined by CFD analysis are shown in Table 6. Wind speeds measured in the winnower test device were lower than those determined by CFD analysis at 9 points by 0 to 2.4 m/s. Figures 10 and 11 show wind speed for actual measurement results of the winnower test device and the CFD analysis to match the top view of Figure 8b. The Kriging method was used. It could predict the attribute value at each point through the linear summation of each measured wind speed based on Table 6 [44]. The minimum unit of the grid was set to be 5.55×5.55 mm and the total number of nodes was set to be 5500. The 0-guide in Figures 10a and 11a showed that wind speed results of the winnower test device and the CFD analysis were high at points C1, C2, and C3 of the discharge port. Wind speeds of the winnower test

device were lower than those of the CFD analysis by 0.1 to 0.7 m/s. As for the 3-guide shown in Figures 10b and 11b, wind speed results of the winnower test device and the CFD analysis showed constant values at distances from 0 to 300 mm from the discharge port. Wind speeds of the winnower test device were lower than those of the CFD analysis at 9 points by 0.1 to 1.6 m/s. Although the 5-guide shown in Figures 10c and 11c had uniform wind speeds at 9 points about the discharge port, and values at L1, C1, and R1 were lower than those of the 3-guide by 1.2 m/s on average. Wind speeds of the winnower test device were lower than those of the CFD analysis at 9 points by 0.4 to 1.8 m/s. The 0-guide shown in Figures 10d and 11d revealed that wind speed results of the winnower test device and the CFD analysis at 1800 RPM were high at points C1, C2, and C3 of the discharge port. Wind speeds of the winnower test device were lower than those of the CFD analysis by 0.8 to 1.2 m/s. As for the 3-guide shown in Figures 10e and 11e, wind speed results of the winnower test device and the CFD analysis had uniform values. Wind speeds of the winnower test device were lower than those of the CFD analysis at 9 points by 0.1 to 2.1 m/s. Although the 5-guide shown in Figures 10f and 11f had uniform wind speeds at 9 points about the discharge port, and values at L1, C1, and R1 were lower than those of the 3-guide by 4.8 m/s on average. Wind speeds of the winnower test device were lower than those of the CFD analysis at 9 points by 0.5 to 2.4 m/s. The 0-guide in Figures 10g and 11g showed that wind speed results of the winnower test device and the CFD analysis at 2000 RPM were high at points C1, C2, and C3 of the discharge port. Wind speeds of the winnower test device were lower than those of the CFD analysis by 0.9 to 1.4 m/s. As for the 3-guide shown in Figures 10h and 11h, wind speed results of the winnower test device and the CFD analysis had uniform values. Wind speeds of the winnower test device were lower than those of the CFD analysis at 9 points by 0.2 to 2.1 m/s. However, the 5-guide shown in Figures 10i and 11i had uniform wind speeds at 9 points about the discharge port, and values at L1, C1, and R1 were lower than those of the 3-guide by 6.3 m/s on average. Wind speeds of the winnower test device were lower than those of the CFD analysis at 9 points by 0.2 to 2.2 m/s, although the 5-guide showed that mean wind speeds at discharge port points L1, C1, and R1 were lower than those of the 3-guide by 6.3 m/s, respectively; the wind speed deviation was reduced by 1.4 m/s. However, as the internal resistance of the winnowing machine generates noise and vibration, additional studies on the way to reduce noise and vibration are required to be conducted.

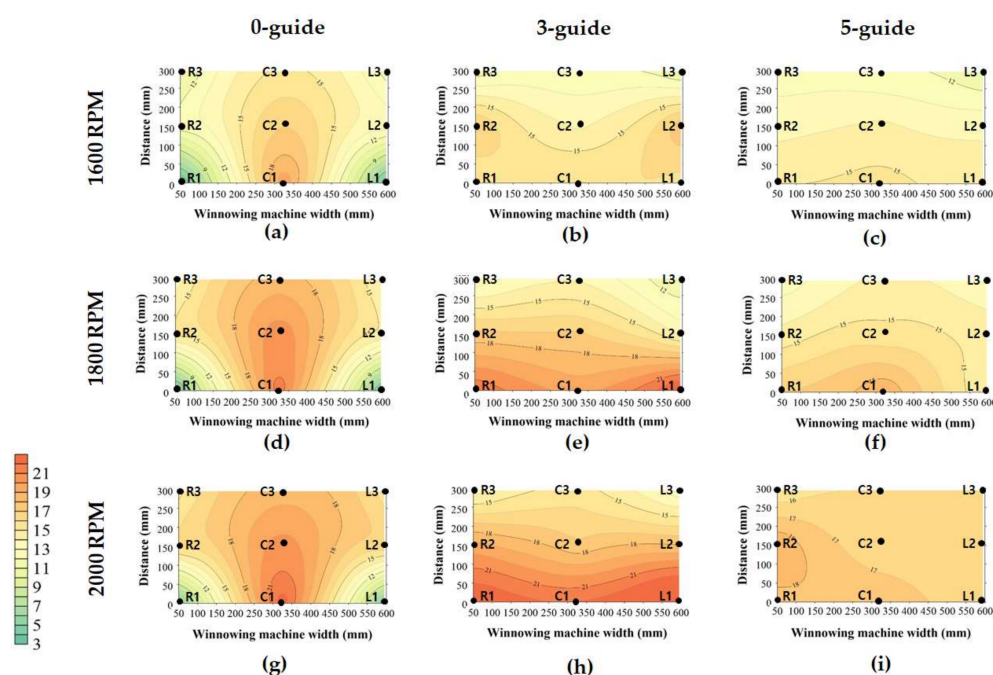


Figure 10. Results of actual measurement for wind velocity on conditions of 0-guide (a), 3-guide (b), and 5-guide (c) at 1600 RPM, 0-guide (d), 3-guide (e), 5-guide (f) at 1800 RPM, and 0-guide (g), 3-guide (h), 5-guide (i) at 2000 RPM.

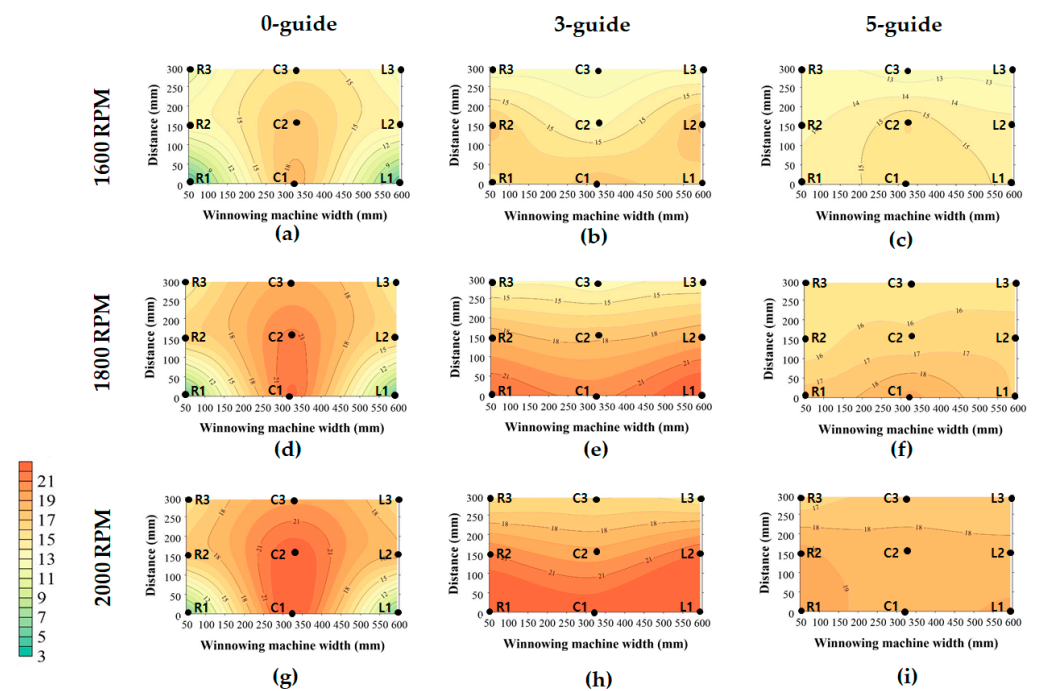


Figure 11. Results of CFD analysis for wind velocity on conditions of 0-guide (a), 3-guide (b), 5-guide (c) at 1600 RPM, and 0-guide (d), 3-guide (e), 5-guide (f), at 1800 RPM, and 0-guide (g), 3-guide (h), 5-guide (i) at 2000 RPM.

Table 6. Experimental results of wind speed by the shape of the winnowing machine and measurement position.

Shape of Winnowing Machine	Distance (mm)	Rotating Speed (RPM)	Measured Value			Analysis Value		
			L1 (m/s)	C1 (m/s)	R1 (m/s)	L1 (m/s)	C1 (m/s)	R1 (m/s)
Existing winnowing machine (0-guide)	0	1600	3.3	19.8	3.6	4.1	19.9	4.4
		1800	3.7	21.6	4.2	4.9	22.6	5.0
		2000	4.9	22.7	4.7	5.8	24.1	5.8
	150	1600	12.6	17.0	13.4	13.8	17.6	14.3
		1800	15.3	20.6	14.8	16.9	21.4	16.2
		2000	16.3	20.5	16.6	17.5	23.2	18.4
	300	1600	10.6	15.2	11.4	11.1	15.5	12.2
		1800	13.4	18.4	13.7	13.8	19.1	14.6
		2000	14.6	18.5	15.4	15.0	19.6	15.8
Winnowing machine with three wind guides (3-guide)	0	1600	14.9	16.1	15.6	15.6	17.7	16.2
		1800	21.9	19.5	23.9	22.3	20.6	24.0
		2000	23.4	22.1	25.8	24.4	22.9	26.8
	150	1600	17.3	13.6	17.8	17.5	13.9	18.3
		1800	17.3	17.2	17.6	18.9	17.8	19.2
		2000	19.5	17.2	18.0	21.1	19.3	20.0
	300	1600	11.2	12.1	10.6	12.1	12.6	12.4
		1800	12.1	13.8	11.0	13.3	14.3	13.1
		2000	13.3	15.6	12.1	15.4	15.8	13.9
Winnowing machine with five wind guides (5-guide)	0	1600	15.0	15.3	14.4	14.2	15.5	14.8
		1800	17.0	18.9	13.9	17.5	19.4	15.9
		2000	17.7	17.9	16.4	19.0	18.6	18.2
	150	1600	13.6	14.2	13.9	13.8	16.1	14.4
		1800	14.4	15.4	14.7	15.0	16.2	16.8
		2000	18.9	16.1	16.1	19.5	18.0	18.3
	300	1600	12.5	12.2	10.9	13.2	12.6	12.3
		1800	12.4	14.3	13.1	14.8	15.6	15.1
		2000	15.1	16.1	16.7	16.1	17.0	17.3

4. Conclusions

The present study measured terminal velocities of chili pepper fruits, branches, and leaves of two species. Aerodynamic analysis of winnower was conducted to develop a foreign material winnower machine to be used after harvesting chili peppers. The performance of the winnower designed through the analysis was validated by conducting a CFD analysis and using a winnower test device. For terminal velocity measurement, species Jeokyoung and AR Legend suitable for mechanical harvesting were used as test samples. An aerodynamic analysis was conducted for chili pepper fruits and chili pepper branches freely falling into a collection tank at different wind speeds. The analysis result showed that chili pepper fruits were collected into the collection tank at a wind speed lower than 17.5 m/s and that chili pepper branches and chili pepper leaves were separated at speeds higher than 12.5 m/s. A winnower was designed using the analysis result. Results of a CFD analysis and a winnower test device were compared to evaluate the rotating speed and the performance of 0-, 3-, and 5-guide at the discharge port. Although the CFD analysis showed that discharged wind speeds were higher than those of the winnower test device by 0 to 2.4 m/s, it was thought to be an effective validation due to the simplification of the design model. As a result of comparing the CFD analysis of the winnower developed in the present study and the performance of the test device, the 3-guide and 5-guide conditions were found to be suitable with a rotating speed of 1800 RPM and a rotating speed of 2000 RPM. However, with the 5-guide, since the winnowing machine generates internal noise and vibration, the guide type must be selected, taking into account the 3-guide or the 5-guide when it is applied to a chili pepper harvester. The winnowing machine developed in this study can be verified through terminal velocity, aerodynamic analysis, CFD flow analysis, testing equipment, and then applied to the chili pepper harvester to reduce the additional workforce in the separation of foreign substances after mechanical harvesting. Therefore, the conditions analyzed in the present study must be verified through additional field tests after applying them to foreign material separation units of chili pepper harvesters.

Author Contributions: Conceptualization, S.-Y.S. and Y.C.; Experiments and data analyses, S.-Y.S. and D.-C.K.; Methodology, M.-H.K.; Writing—original draft preparation, S.-Y.S. and Y.C.; Project administration, Y.C.; Writing—review and editing, Y.C., D.-C.K. and M.-H.K. All authors have read and agreed to the published version of the manuscript.

Funding: This work was supported by a grant (716001-7) of the Korea Institute of Planning and Evaluation for Technology in Food, Agriculture, and Forestry (IPET) through the Agriculture, Food, and Rural Affairs Convergence Technologies Program for Educating Creative Global Leader Program funded by the Ministry of Agriculture, Food, and Rural Affairs (MAFRA), Republic of Korea. It was also supported by a grant (NRF-2021R1G1A1012778) of the National Research Foundation of Korea (NRF) funded by the Korean government (MSIT, Ministry of Science and ICT). This research was supported by “Research Base Construction Fund Support Program” funded by Jeonbuk National University in 2022.

Institutional Review Board Statement: Not applicable.

Informed Consent Statement: Not applicable.

Data Availability Statement: Not applicable.

Conflicts of Interest: The authors declare no conflict of interest.

References

1. Food and Agriculture Organization-World Health Organization. Production Share of Chilies and Peppers, Dry by Region. Available online: <https://www.fao.org/faostat/en/#data/QCL/visualize> (accessed on 12 January 2022).
2. Statistics Korea. Production of Chili Pepper. Available online: <http://kostat.go.kr/portal/eng/pressReleases/1/index.board?bmode=read&aSeq=415243> (accessed on 12 January 2022).
3. Statistics Korea. Current State of Farm Mechanization. Available online: http://www.index.go.kr/potal/main/EachDtlPageDetail.do?idx_cd=1288 (accessed on 7 February 2022).

4. Funk, P.A.; Walker, S.J. Evaluation of five green chili cultivars utilizing five different harvest mechanisms. *Appl. Eng. Agric.* **2010**, *26*, 955–964. [[CrossRef](#)]
5. Chen, Y.C.; Kong, L.J.; Wang, H.X. Research of mechanism and experiment of 4LZ-3.0 self-propelled pepper harvester. *Appl. Mech. Mater.* **2013**, *419*, 217–222. [[CrossRef](#)]
6. Nishanth, M.S.; Jayan, P.R.; Pankaj, M.; Ratnakiran, D.W. Design, development and evaluation of pepper harvester. *J. AgriSearch* **2020**, *7*, 82–85. [[CrossRef](#)]
7. Walker, S.J.; Funk, P.A. Mechanical harvest trials of New Mexican-type green chile (*Capsicum annuum* L.). *Hort. Sci.* **2010**, *45*, 145–146.
8. Calsoyas, I.; Walker, S.; Funk, P. Comparison of Six Green Chile (*Capsicum annuum* L.) Cultivars on Harvest Efficiency with Etgar[®] Picker. In Proceedings of the Annual Meeting of the American Society for Horticultural Science, Philadelphia, PA, USA, 3–7 January 2016; Volume 51, pp. 267–268.
9. Nam, J.S.; Kang, Y.S.; Kim, S.B.; Kim, D.C. Factorial experiment for drum-type secondary separating part of self-propelled pepper harvester. *J. Biosyst. Eng.* **2017**, *42*, 242–250. [[CrossRef](#)]
10. Shin, S.-Y.; Kim, M.-H.; Cho, Y.; Kim, D.-C. Performance testing and evaluation of drum-type stem separation device for pepper harvester. *Appl. Sci.* **2021**, *11*, 9225. [[CrossRef](#)]
11. Marshall, D.E. Mechanized pepper harvesting and trash removal. In Proceedings of the First International Conference on Fruit, Nut and Vegetable Harvesting Mechanization, Bet Dagan, Israel, 5–12 October 1983; American Society of Agricultural and Biological Engineers: St. Joseph, MI, USA, 1984; Volume 5, pp. 276–279.
12. Esch, T.A.; Marshall, D.E. Trash removal from mechanically harvested peppers. *Trans. ASAE* **1987**, *30*, 893–898. [[CrossRef](#)]
13. Funk, P.A.; Marshall, D.E. Pepper Harvest Technology. In *Peppers: Botany, Production and Uses*; Russo, V.M., Ed.; CABI: Wallingford, UK, 2012; pp. 227–240. [[CrossRef](#)]
14. Kim, T.-H.; Kim, D.-C.; Cho, Y. Performance comparison and evaluation of two small chili pepper harvester prototypes that attach to walking cultivators. *Appl. Sci.* **2020**, *10*, 2570. [[CrossRef](#)]
15. Lenker, D.H.; Nascimento, D.F. Mechanical harvesting and cleaning of chili peppers. *Trans. ASAE* **1982**, *25*, 42–46. [[CrossRef](#)]
16. Wolf, I.; Alper, Y. Mechanization of Paprika Harvest. In Proceedings of the First International Conference on Fruit, Nut and Vegetable Harvesting Mechanization, Bet Dagan, Israel, 5–12 October 1983; American Society of Agricultural and Biological Engineers: St. Joseph, MI, USA, 1984; Volume 5, pp. 265–275.
17. Eaton, F.E.; Wilson, C. *Refinement and Testing of Mechanical Cleaners for Red Chile*. New Mexico State University Chile Task Force Report 22; New Mexico State University Library: Las Cruces, NM, USA, 2005.
18. Kong, L.; Chen, Y.; Ma, L.; Duan, Y. Research and design of line pepper' cleaning and separating device, based on star wheel and airflow. *J. Chin. Agri. Mech.* **2013**, *34*, 102–105.
19. Jo, Y.J.; Kang, Y.S.; Nam, J.S.; Choe, J.S.; Inoue, E.; Okayasu, T.; Kim, D.C. Performance analysis for a card cleaner type separating system of pepper harvester. *J. Fac. Agric. Kyushu-Univ.* **2018**, *63*, 103–111. [[CrossRef](#)]
20. Byum, J.H.; Nam, J.S.; Choe, J.S.; Inoue, E.; Okayasu, T.; Kim, D.C. Analysis of the separating performance of a card cleaner for pepper harvester using EDEM software. *J. Fac. Agric. Kyushu-Univ.* **2018**, *63*, 347–354. [[CrossRef](#)]
21. Bilanski, W.K.; Collins, S.H.; Chu, P. Aerodynamic properties of seed grains. *Agric. Eng.* **1962**, *43*, 216–219.
22. Lee, C.H.; Cho, Y.J.; Kim, M.S. Aerodynamic Study on Pneumatic Separation of Grains(I) -An Experimental Study on The Vertical Wind Tunnel-. *J. Biosyst. Eng.* **1989**, *14*, 272–281.
23. Lee, C.H.; Cho, Y.J.; Kim, M.S. Aerodynamic Study on Pneumatic Separation of Grains(II) -The Measurement of the Terminal Velocities of Grains-. *J. Biosyst. Eng.* **1990**, *15*, 1–13.
24. Chung, C.J.; Nam, S.I.; Joo, B.C. Pneumatic Separation on Separating Unit of a Combine Harvester. *J. Biosyst. Eng.* **1988**, *13*, 32–43.
25. Kim, M.H.; Park, S.J.; Noh, S.H. Study on the Physical, Mechanical and Aerodynamic Properties of Peanut Pods. *J. Biosyst. Eng.* **1995**, *20*, 141–150.
26. Choi, Y. Development of Machine Harvester for Pepper. Ph.D. Thesis, Chonnam National University, Gwangju, Korea, 2006.
27. Hong, J.T.; Cho, K.H.; Cho, N.H.; Park, H.M.; Hong, S.K.; Choi, Y.; Shin, S.Y.; Cho, C.K. Study on Integrated Mechanization System for Harvest and Postharvest Operation of Once-over-harvest Pepper. In Proceedings of the Korean Society for Agricultural Machinery Conference, Suwon-si, Korea, 17–18 November 2006.
28. Noh, H.K.; Han, D.W.; Lee, E.S.; Kang, T.H. Effect of air blast velocity for separating efficiency of sesame thresher. In Proceedings of the Korean Society for Agricultural Machinery, Yesan-gun, Korea, 2–3 May 2013.
29. Lee, J.S.; Kim, B.J.; Kang, Y.S.; Kim, D.C. Analysis of flow for peanut harvest fan system using CFD. In Proceedings of the Korean Society for Agricultural Machinery, Jeju-si, Korea, 1–2 November 2013.
30. Kim, B.J.; Kang, Y.S.; Kim, H.G.; Inoue, E.; Okayasu, T.; Kim, D.C. Analysis of the separating performance of peanut harvester sorting system. *J. Fac. Agric. Kyushu-Univ.* **2015**, *60*, 209–214. [[CrossRef](#)]
31. Yuan, J.; Li, H.; Qi, X.; Hu, T.; Bai, M.; Wang, Y. Optimization of airflow cylinder sieve for threshed rice separation using CFD-DEM. *Eng. Appl. Comp. Fluid. Mech.* **2020**, *14*, 871–881. [[CrossRef](#)]
32. Shin, S.Y.; Kim, D.C.; Kang, Y.S.; Cho, Y. Factorial experiment for air blower of the pepper harvester. *J. Biosyst. Eng.* **2020**, *45*, 239–248. [[CrossRef](#)]
33. Zhao, J.; Sugirbay, A.; Liu, F.; Chen, Y.; Hu, G.; Zhang, E.; Chen, J. Parameter optimization of winnowing equipment for machine-harvested *Lycium barbarum* L. *Span. J. Agric. Res.* **2019**, *17*, e0203. [[CrossRef](#)]

34. Franco, A.; Valera, D.L.; Pena, A.; Pérez, A.M. Aerodynamic analysis and CFD simulation of several cellulose evaporative cooling pads used in Mediterranean greenhouses. *Comput. Electron. Agric.* **2011**, *76*, 218–230. [[CrossRef](#)]
35. Doushtaghi, M.H.; Minaei, S.; Khoshtaghaza, M.H. Computational fluid dynamics and analytical modeling for predicting effects of airflow temperature and relative humidity on the terminal velocity of agricultural granular materials. *J. Food Process Eng.* **2022**, *45*, e13941. [[CrossRef](#)]
36. Di Perta, E.S.; Agizza, M.A.; Sorrentino, G.; Boccia, L.; Pindozi, S. Study of aerodynamic performances of different wind tunnel configurations and air inlet velocities, using computational fluid dynamics (CFD). *Comput. Electron. Agric.* **2016**, *125*, 137–148. [[CrossRef](#)]
37. Garrett, R.E.; Brooker, D.B. Aerodynamic drag of farm grains. *Appl. Eng. Agric.* **1965**, *26*, 45–52. [[CrossRef](#)]
38. Song, H.; Litchfield, J.B. Predicting method of terminal velocity for grains. *Appl. Eng. Agric.* **1991**, *34*, 225–231. [[CrossRef](#)]
39. Chakraverty, A.; Singh, R. *Postharvest Technology and Food Process Engineering*; CRC Press: Boca Raton, FL, USA, 2014.
40. Meriam, J.L.; Kraige, L.G. *Engineering Mechanics—Dynamics*, 9th ed.; John Wiley & Sons, Inc.: Hoboken, NJ, USA, 2020.
41. ANSYS Inc. *FLUENT Manual—ANSYS 2020 Version R1, Theory Guide*; ANSYS Inc.: Canonsburg, PA, USA, 2020.
42. Lee, M.-H.; Kang, Y.-S.; Kim, D.-C.; Choi, Y. A Study on the Performance Improvement of Foreign Materials Separating System for a Pepper Harvester. *J. Agric. Life Sci.* **2020**, *54*, 111–120. [[CrossRef](#)]
43. ANSYS Inc. *FLUENT Training Material—ANSYS 2020 Version R1, Lecture Transient Flow Modeling, Introduction to ANSYS Fluent*; ANSYS Inc.: Canonsburg, PA, USA, 2020.
44. Oliver, M.A.; Webster, R. Kriging: A method of interpolation for geographical information systems. *Int. J. Geogr. Inf. Syst.* **1990**, *4*, 313–332. [[CrossRef](#)]